Article

Journal of
Nanoscience and Nanotechnology
Vol. 14, 9680–9685, 2014
www.aspbs.com/jnn

Effect of RF Pulsing Biasing on the Etching of Magnetic Tunnel Junction Materials Using CH_3OH

Min Hwan Jeon[1], Deok Hyun Yun[2], Kyung Chae Yang[2], Ji Youm Youn[1], Du Yeong Lee[3], Tae Hun Shim[3], Jea Gun Park[3], and Geun Young Yeom[1, 2, *]

[1] *SKKU Advanced Institute of Nano Technology (SAINT), Sungkyunkwan University, Suwon, Gyeonggi-do 440-746, South Korea*
[2] *Department of Materials Science and Engineering, Sungkyunkwan University, Suwon, Gyeonggi-do 440-746, South Korea*
[3] *Department of Electronics Engineering, Hanyang University, Seoul 133-791, South Korea*

The magnetic tunnel junction (MTJ)-related materials such as CoFeB, CoPt, MgO, and Ru, and W were etched using CH_3OH in a pulse-biased inductively coupled plasma system and the effect of bias pulsing (100% ~ 30% duty percentage) on the etch characteristics of the MTJ-related materials was investigated at the substrate temperature of 200 °C. The etch selectivity of MTJ-related materials over W was improved by using pulse-biasing possibly due to the formation of more stable and volatile etch products during the pulse-off time and the removal of the compounds more easily on the etched CoFeB surface during the pulse-on time. X-ray photoelectron spectroscopy also showed that the use of lower duty percentage decreases the residue thickness remaining on the etched MTJ materials indirectly indicated the higher volatility of the etch products by the bias pulsing. The etching of nano-patterned CoFeB masked with W also showed more anisotropic etch profile by pulse-biasing probably due to the increased the etch selectivity of CoFeB over W and the decreased redeposition of etch products on the sidewall of the CoFeB features. The most anisotropic CoFeB etch profiles could be observed by using CH_3OH gas in the pulse biasing of 30% duty ratio.

Keywords: Magnetic Tunnel Junction Materials, Etch Characteristics, Pulse Biased Icp, Substrate Heating, CH_3OH Gas.

1. INTRODUCTION

Among the many non-volatile memory devices, magnetic random access memory (MRAM) device is one of the most promising candidates for the next generation memory devices. MRAM device has fast access time, high storage density, low operating voltage, infinite rewrite capability comparing to conventional memory devices.[1–3] Especially, spin transfer torque (STT) MRAM has the characteristics that are applicable to highly integrated circuit due to the lower required current density in the operation of the device. It is believed that STT-MRAM can not only replace (static RAM) SRAM/flash memory and battery-backed up RAM but also supply improved non-volatile memory solutions for high-end smart electronic devices.[4–7]

For the fabrication of highly integrated STT-MRAM, dry etch process is very important issue due to the difficulty in the formation of volatile etch byproducts between the ferromagnetic materials and etch gases. At first, Ar ion milling method has been applied to etch the MTJ stacks. However, the redeposition of the back-sputtered etch byproducts on the sidewall, the low etch rate and etch damage are disadvantages of this method.[8, 9] Halogen-based plasma etching tends to show several etch problems such as the non-volatile etch byproducts remaining on the pattern sidewall, the chemical damage caused by residual corrosion, etc.[10–12] To overcome these etch problems, several etch chemistries such as CO/NH_3, CH_3OH gases which probably increase the volatility of etch byproducts have been intensively investigated.[13–18] However, the volatility of etch byproducts is not high due to low chemical reaction between etchant gases and MTJ materials even though these reactive gases were used in the conventional plasma etching method.

In the previous study, to increase the formation of the volatile metal carbonyl compounds for highly selective etching of MTJ materials over W, a pulse-biased

*Author to whom correspondence should be addressed.

 1533-4880/2014/14/9680/006 doi:10.1166/jnn.2014.10185

inductively coupled plasma (ICP) technique has been investigated by using CO/NH_3 gas combination and pulsed radio frequency (rf) power to the substrate.[19] By using the pulse-biased ICP technique, the etch characteristics of MTJ materials were improved with decreasing the pulse duty percentage probably due to the formation of the more volatile and more stable etch compounds during the pulse-off time. Also, another research group investigated the effect of substrate heating up to 120 °C on the etching of MTJ materials using CH_3OH gas in a conventional ICP system. The etch rates of MTJ materials at the elevated substrate temperature gradually increased even though they concluded that the increase of MTJ etch rate is more responsible for the formation of pure metal at the elevated temperature rather than the formation of volatile and stable etch compounds.[20]

In this study, the etch characteristics of MTJ-related materials such as CoPt, CoFeB, MgO, W and patterned MTJ stack have been studied by using CH_3OH gas in the rf bias pulsing with substrate heating. These effects were investigated to examine the possible formation of volatile metal carbonyl related compounds.

2. EXPERIMENTAL CONFIGURATION

For the etching of MTJ-related materials, CoFeB, CoPt, MgO, and a hard mask material such as W were prepared to investigate the etch characteristics by various pulsed bias conditions with substrate heating to 200 °C using CH_3OH in an inductively coupled plasma (ICP) system. The ICP etch system used in this experiment is an eight-inch diameter commercial etcher (STS PLC, UK) and the schematic diagram of the pulse-biased ICP system is shown in Figure 1. As shown in this figure, one-turn inductive coil was wound around the ceramic chamber wall and a 13.56 MHz rf generator was connected to the inductive coil. Also, a separate 13.56 MHz rf power was applied to the substrate for rf pulse biasing, and the substrate was heated to 200 °C using an oil heater (P5, LAUDA). A separate 13.56 MHz pulsed rf power was applied to the substrate using a pulse/function generator (8116A, HP), a signal generator (8657B, HP), and an rf power amplifier (A1000, ENI).

Blank MTJ-related materials such as CoFeB, CoPt, MgO, and blank W were used to investigate the etch characteristics such as etch rate and etch selectivity. Also, 21 nm thick MTJ stack which is consisted of CoPt/MgO/CoFeB deposited on a Ta/Silicon wafer and patterned with W(100 nm)/Ru(5 nm) was used to investigate the MTJ etch profiles. These materials and patterned MTJ stack were etched using CH_3OH gas with the gas flow rate of 30 sccm and the process pressure of 5 mTorr. The 13.56 MHz ICP source power of 500 W and DC bias voltage of −300 V (time-averaged DC bias voltage) were used to etch the MTJ-related materials and patterned MTJ stack. During the pulsed rf biasing, time-averaged DC biasing was used to compensate the decrease of etch rates by the pulsing.[19]

To measure the etch depth of etched MTJ materials, a step profilometer (Alpha step 500, Tencor) was used. Also, the etched CoFeB samples were investigated using X-ray photoelectron spectroscopy (XPS, ESCA2000, VG Microtech Inc.) and the chemical bonding characteristics of the residue remaining on the CoFeB surface were studied using a Mg $K\alpha$ twin-anode source. The surface morphology of CoFeB and MgO after the etching was analyzed with an atomic force microscope (AFM, SPA-300HV). The etch profile of the patterned MTJ stack on a Ta/silicon wafer was observed by using a field emission scanning electron microscope (FE-SEM, Hitachi S-4700).

3. RESULTS AND DISCUSSION

Figure 2 shows the etch rates of MTJ-related materials (CoFeB, CoPt, MgO, and Ru) and W and the etch selectivities of MTJ-related materials over W as a function of pulse duty percentage. For the etching, the 13.56 MHz rf power to the ICP source was maintained at 500 W and the substrate voltage was kept at −300 V dc (time-average DC bias voltage). The operating pressure was 5 mTorr while maintaining the CH_3OH gas flow rate at 30 sccm. For the substrate temperature, the increase of substrate temperature generally increased the etch rates of MTJ-related materials and the etch selectivities over W, therefore, we kept the substrate temperature at 200 °C in this experiment. The pulse duty percentage of the substrate rf power was varied while maintaining the pulse frequency at 50 kHz. As shown in Figure 2(a), when the materials were etched with CW (100%) biasing, the etch rate of the MTJ-related materials was the highest for CoPt and it was followed by CoFeB, Ru, and MgO. The etch rate of W was the lowest. When the duty percentage of the substrate biasing was decreased from CW to 30%, the etch rates of MTJ-related materials and W were decreased with decreasing

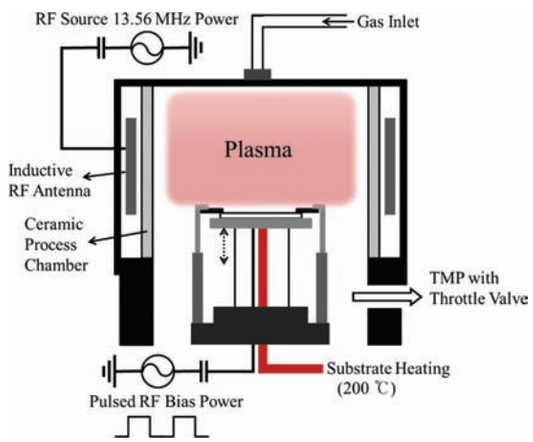

Figure 1. Schematic diagram of the inductively coupled plasma etcher used in this study.

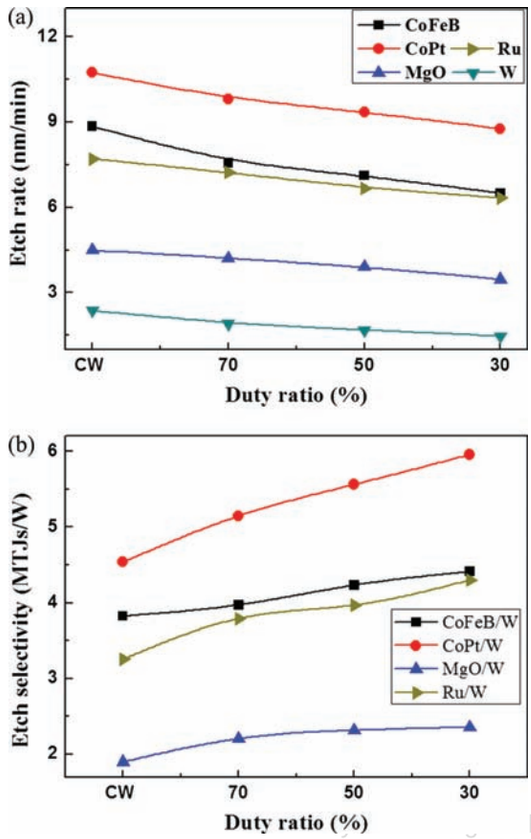

Figure 2. Etch rate of MTJ materials and W, and etch selectivities of MTJ materials over W using CH_3OH gas as a function of pulse duty percentage. (a) etch rates of MTJ materials and W, (b) etch selectivities of MTJ materials over W.

the duty percentage but were not significantly decreased with decreasing the pulse duty percentage due to the use of time averaged dc biasing (that is, for 50% duty percentage, −600 V of DC bias voltage was used when −300 V was used for the CW biasing to have the time averaged DC bias voltage of −300 V.) However, the etch selectivities of MTJ-related materials over W were improved with the decrease of duty percentage and, at 30% of duty percentage, the etch selectivities of CoPt/W, CoFeB/W, Ru/W, and MgO/W were 6.0, 4.4, 4.3, and 2.4, respectively. The increased etch selectivities over W appear to be related to the formation of more volatile compounds during the pulse-off time and the removal of the compound more easily during the pulse-on time.

Using CoFeB, the chemical bonding states of the residue remaining on the MTJ-related material surface during the etching using CH_3OH were investigated by XPS for the rf CW biasing and the rf pulse biasing at 30% duty percentage (50 kHz duty frequency). Other etch conditions are the same as those in Figure 2. Figure 3 shows the XPS narrow scan data of Co 2*p*, Fe 2*p*, and B 1*s* measured as a function of sputter time using an Ar^+ ion gun (3 keV ion energy and 2 μA ion current) for the XPS depth profiling of the CoFeB etched with the rf CW biasing and the rf pulse biasing at 30% duty percentage. The surface of the etched CoFeB was sputter etched for 360 sec and the surface was measured by XPS repeatedly after each 90 sec of sputter etching. The XPS binding energies before the etching were of 778.3 and 793.2 eV for Co 2*p*, 707 and 720.2 eV for Fe 2*p*, 188 eV for B 1*s*. After the etching, as shown in Figure 3, additional peaks at 781 and 797.1 eV for Co 2*p*, 710 and 723.5 eV for Fe 2*p*, and 192 eV for B 1*s* were observed. The observation of the additional higher binding energy peaks appears to be related to the Co–O (or CO), Fe–O (or CO), and B–O (or CO) caused by the oxygen and CO dissociated from CH_3OH and both CoFeB samples etched by the rf CW biasing and the rf pulse biasing showed the same additional peaks. However, the depth profiling showed that the CoFeB etched by the rf CW biasing took longer sputter time to recover pure CoFeB surface compared that etched by the rf pulse biasing of 30% duty percentage even though the differences were not significant.

The change of relative atomic percentages of the CoFeB surfaces etched by rf CW biasing and rf pulse biasing (30%) during the depth profiling in Figure 3 was measured and the results are shown in Figure 4. Before the etching, the relative atomic percentage of Co:Fe:B was 51%:36%:13%. As shown in the figure, before the depth profiling, the surface of the etched CoFeB was composed of mostly carbon and oxygen in addition to a low percentage of Co, Fe, and B possibly due to the formation of CO compounds remaining on the etched CoFeB surface. The carbon and oxygen were decreased rapidly and Co, Fe, and B were increased slowly with the increase of sputter etch time for both CoFeB samples etched by the rf CW biasing and the rf pulse biasing of 30% duty percentage. However, the CoFeB etched by the rf CW biasing took about 360 sec sputter time to recover the stoichiometric CoFeB composition while that etched by the rf pulse biasing recovered the pure CoFeB composition after 180 sec. Therefore, the residue remaining on the CoFeB surface etched by the rf CW biasing was thicker than that etched by rf pulse biasing. The thinner residue thickness remaining after the etching of CoFeB by the rf pulse biasing compared to that by the rf CW biasing using CH_3OH appears to be related to the easier formation of volatile etch compounds such as metal carbonyls during the pulse-off time and the easier removal of those etch products during the pulse-on time by the rf pulse biasing.

The surface roughness of CoFeB and MgO etched by the rf CW biasing and the rf pulse biasing with the duty percentages of 70, 50, and 30% was measured using AFM and the results are shown in Figure 5. As a reference, the surface roughness of as-received CoFeB and MgO was also measured. The etch conditions are the same as those in Figure 2. As shown, the surface roughness of as-received CoFeB and MgO was 0.81 nm and 1.26 nm, respectively. After the etching of CoFeB and MgO, the

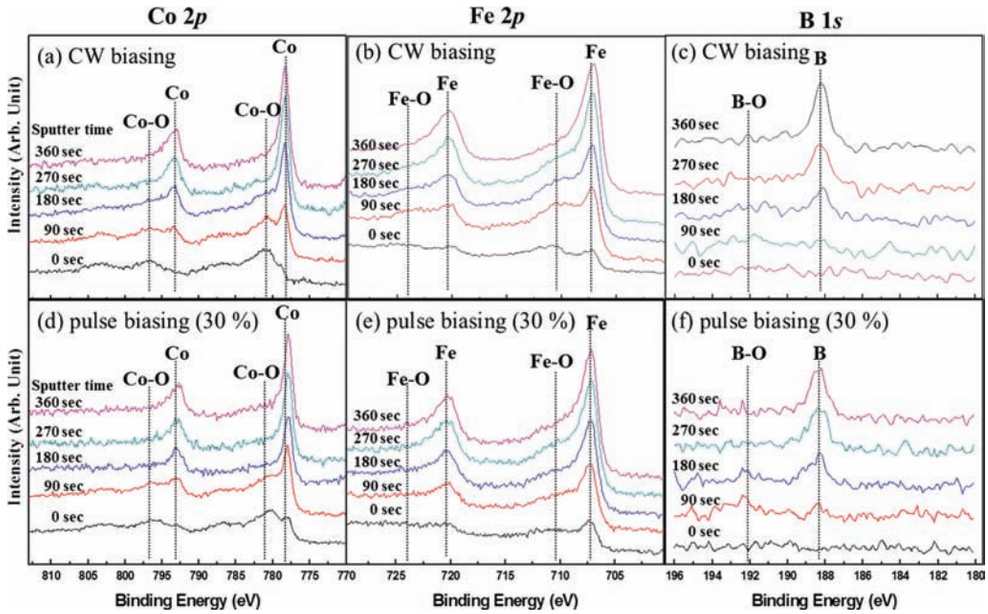

Figure 3. XPS narrow scan data of (a) Co 2*p*, (b) Fe 2*p*, and (c) B 1*s* during the depth profiling of the etched CoFeB surface for the etching using the rf CW biasing and rf pulse biasing with the duty percentage of 30%. The CoFeB sample was etched using CH_3OH gas with substrate temperature of 200 °C for three minutes.

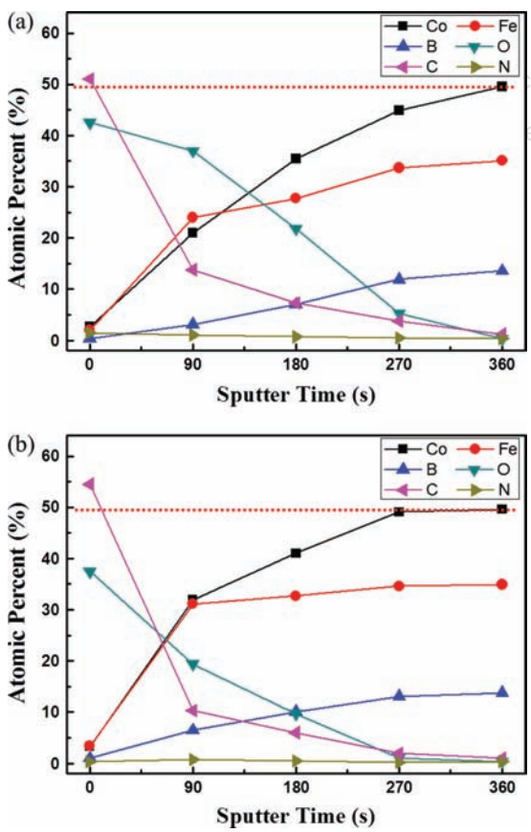

Figure 4. Relative atomic percentages of the etched CoFeB measured by XPS depth profiling as a function of Ar^+ ion depth profiling time for CoFeB samples etched using CH_3OH gas by (a) rf CW biasing and (b) rf pulse biasing of 30% duty percentage.

surface roughness was increased regardless of etch conditions, however, the surface roughness of CoFeB and MgO etched by the rf CW (100%) biasing showed the highest surface roughness of 3.93 nm and 6.39 nm. By rf pulse biasing the substrate from 100 to 30%, the surface roughness was decreased for both CoFeB and MgO and, when 30% of rf pulse biasing was used, the surface roughness of CoFeB and MgO was decreased to 1.56 nm and 3.27 nm, respectively. The smoother CoFeB and MgO surfaces after the rf pulse biasing and at the lower duty percentage appear to be related to the uniform chemical reaction (especially for CoFeB, for MgO there is no known volatile carbonyl compounds, therefore, MgO is generally sputter etched.) during the pulse-off time and the nonselective removal of the reacted species with higher instant ion energy with decreasing duty percentage. For CoFeB, the higher substrate temperature also showed lower surface roughness at the same rf biasing condition possibly due to the increased chemical reaction between CH_3OH and CoFeB and the increased removal of the chemically reacted materials (not shown).

The MTJ stack consisted of CoPt(10 nm)/MgO(1 nm)/CoFeB(10 nm) deposited on a Ta/Silicon wafer and patterned with W(100 nm)/Ru(5 nm) was etched and the etch profiles of the MTJ stack were observed by FE-SEM and the results are shown in Figure 6. For the etching of the MTJ stack, 500 W of the 13.56 MHz was applied to the ICP source and −300 V of time-averaged DC bias voltage to the substrate by using a separate 13.56 MHz rf power. The pulse duty percentage to the substrate was varied from 100% (CW) to 30% while the duty frequency was fixed at

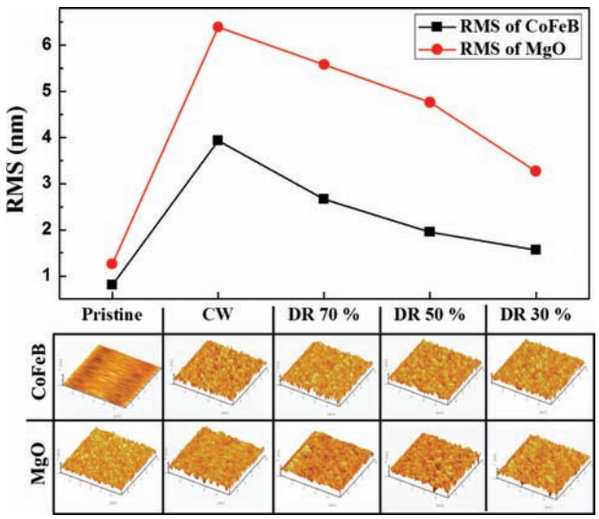

Figure 5. AFM surface roughness of the etched CoFeB and MgO using CH_3OH gas as a function of rf pulse duty percentage. As references, the surface roughness measured for pristine CoFeB and MgO was included.

50 kHz. The operating pressure was 5 mTorr with 30 sccm of CH_3OH. The substrate temperature was kept at 200 °C. As shown in the figure, for the MTJ stack etched by the rf CW (100%) biasing, due to a thick sidewall residue formation during the MTJ stack etching using CH_3OH, the gap between the MTJ stack feature was decreased and even merged for the small gap between two MTJ stack features. As the rf pulse duty percentage is decreased to 70, 50, and 30%, the MTJ stack feature became slimmer and the gap between the MTJ stack was increased, and at 30% of rf pulse duty percentage, the most anisotropic MTJ stack etch profile could be obtained. The improved MTJ etch profile with less residue on the sidewall of the etched feature by using the rf pulse biasing and with decreasing the rf pulse duty percentage is believed to be related to the stable volatile carbonyl compound formation during the pulse-off time and the easier removal of those compounds without severe redeposition on the sidewall of the feature during the pulse-on time. Also, it is known that, for the sputter etching, with increasing the ion bombardment energy, the sputtered flux on the substrate changes from undercosine distribution to overcosine distribution. In our experiment, time-averaged DC biasing was used, therefore, the instant DC bias voltage is increased with decreasing the pulse duty percentage at the same time-averaged DC biasing, therefore, less sputtered materials are redeposited on the sidewall of the etched feature at the higher ion bombardment energy. Therefore, by decreasing the sidewall redeposition in addition to the stable volatile compound formation (except for MgO), more anisotropic MTJ stack etch profile could be obtained by using the rf pulse bias condition.

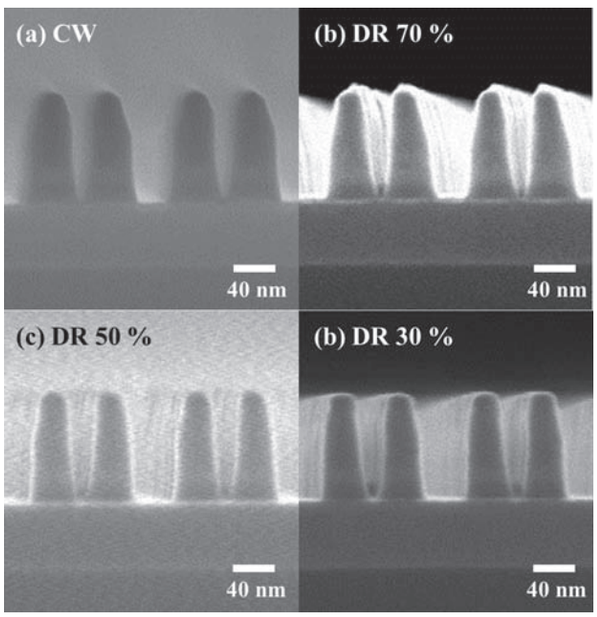

Figure 6. FE-SEM images of the etched CoFeB as a function of rf pulse duty percentage. 21 nm thick MTJ stack composed of CoPt(10 nm)/MgO(1 nm)/CoFeB(10 nm) was deposited on a Ta/silicon wafer and patterned with W hard mask. (a) CW, (b) duty percentage of 70%, (c) duty percentage of 50% and (d) duty percentage of 30%.

4. CONCLUSIONS

MTJ materials such as CoFeB, CoPt, MgO, and Ru and the hard mask material such as W were etched using CH_3OH gas in a pulse-biased ICP system while substrate heating at 200 °C and the etch characteristics of MTJ-related materials were investigated as a function of pulse duty percentage. By rf pulse biasing the substrate, the etch selectivity of MTJ materials over W was gradually increased possibly due to the formation of stable volatile carbonyl-related compounds between MTJ-related materials and CH_3OH except for MgO. In the etching of blank CoFeB using CH_3OH gas, the thickness of the etch residue remaining on the CoFeB surface and the surface roughness were decreased with the decrease of pulse duty percentage, and it is believed to be related to the formation of volatile carbonyl compounds uniformly on the CoFeB surface during the pulse-off time and non-selective removal of the reacted species during the pulse-on time. The improved etch profile of a MTJ stack consisted of CoPt/MgO/CoFeB could be obtained at the lower pulse duty percentage possibly due to the formation of more stable and volatile metal carbonyls during the pulse-off time and the decreased redeposition on the sidewall of the MTJ feature for the higher instant ion bombardment energy during the pulse-on time. As a result, the most anisotropic etch profile of MTJ stack could be observed by using the rf pulse biasing of 30% duty percentage while etching using CH_3OH gas and the time-averaged DC bias voltage condition.

Acknowledgments: This work was supported by the SRC project No. 2011-IN-2219. The authors would like to

thank Dr. Satyarth Suri and Dr. Bob Turkot in Intel Corp. for helpful discussion on MRAM etching.

References and Notes

1. K. Kim and G. H. Koh, *Proc. 24th Int. Conf. Microelectronics* (**2004**), p. 377.
2. G. Muller, T. Happ, M. Kund, G. Y. Lee, N. Nagel, and R. Sezi, *IEDM Tech. Dig.* (**2004**), p. 567.
3. R. C. Sousa and I. L. Prejbeanu, *C. R. Physique* 6, 1013 (**2005**).
4. H. Kubota, A. Fukushima, Y. Otani, S. Yuasa, K. Ando, H. Maehara, K. Tsunekawa, D. D. Djayaprawira, N. Watanabe, and Y. Suzuki, *Jpn. J. Appl. Phys.* 44, L1237 (**2005**).
5. S. Mangin, D. Ravelosona, J. A. Katine, M. J. Carey, B. D. Terris, and E. E. Fullerton, *Nat. Mater.* 5, 210 (**2006**).
6. J. Hayakawa, S. Ikeda, Y. M. Lee, R. Sasaki, T. Meguro, F. Matsukura, H. Takahashi, and H. Ohno, *IEEE Trans. Magn.* 44, 1962 (**2008**).
7. S. Ikeda, K. Miura, H. Yamamoto, K. Mizunuma, H. D. Gan, M. Endo, S. Kanai, J. Hayakawa, F. Matsukura, and H. Ohno, *Nat. Mater.* 9, 721 (**2010**).
8. H. R. Liua, B. J. Qua, T. L. Rena, L. T. Liua, H. L. Xieb, and C. X. Lib, *J. Magn. Magn. Mater.* 267, 386 (**2003**).
9. T. Seki, T. Shima, K. Takanashi, Y. Takahashi, E. Matsubara, and Y. K. Takahashi, *J. Appl. Phys.* 96, 2 (**2004**).
10. J. M. Francou, A. Inard, and D. Henry, *Microelectron Eng.* 13, 425 (**1991**).
11. C. G. C. H. M. Fabrie, J. T. Kohlhepp, H. J. M. Swagten, B. Koopmans, M. S. P. Andriesse, and E. Vander Drift, *J. Vac. Sci. Technol. B* 24, 2627 (**2006**).
12. K. B. Jung, E. S. Lambers, J. R. Childress, S. J. Pearton, M. Jenson, and A. T. Hurst, *Appl. Phys. Lett.* 71, 1255 (**1997**).
13. T. Osada, M. Doi, K. Sakamoto, H. Maehara, and Y. Kodaira, *Proc. 26th Int. Symp. Dry Process (DPS)* (**2004**), p. 127.
14. X. Peng, S. Wakeham, A. Morrone, A. Axdal, M. Feldbaum, J. Hwu, T. Boonstra, Y. Chen, and J. Ding, *Vacuum* 83, 1007 (**2009**).
15. H. Kubota, K. Ueda, Y. Ando, and T. Miyazaki, *J. Magn. Magn. Mater.* 272–276, E1421 (**2004**).
16. A. S. Orland and R. Blumenthal, *J. Vac. Sci. Technol. B* 23, 1597 (**2005**).
17. X. Kong, D. Krasa, H. P. Zhou, W. Williams, S. McVitie, J. M. R. Weaver, and C. D. W. Wilkinson, *Microelectron. Eng.* 85, 988 (**2008**).
18. K. Kinoshita, T. Yamamoto, H. Honjo, N. Kasai, S. Ikeda, and H. Ohno, *Jpn. J. Appl. Phys.* 51, 08HA01 (**2012**).
19. M. H. Jeon, H. J. Kim, K. C. Yang, S.-K. Kang, K. N. Kim, and G. Y. Yeom, *Jpn. J. Appl. Phys* 52, 05EB03 (**2013**).
20. M. S. Lee and W. L. Lee, *Appl. Surf. Sci* 258, 8100 (**2012**).

Received: 27 January 2014. Accepted: 12 April 2014.